

Comparative Study of Impact Simulation Models for Linear Elastic Structures in Seismic Pounding



N. U. Mate¹, S. V. Bakre² and O. R. Jaiswal³

¹Research Scholar, ²Associate Professor, ³Professor

Applied Mechanics Department,

Visvesvaraya National Institute of Technology, Nagpur, Maharashtra, India-440 010

SUMMARY:

This paper presents a comparative study of various existing linear and non-linear simulation models for pounding on three adjacent single-degree-freedom and multi-degree-freedom linear elastic structures. The prediction of impact response of structure is done by means of spring-dashpot contact element, which will be activated only when the bodies comes in contact. The present work is carried out on FE based software tool SAP 2000 NL and MATLAB solver considering three different real earthquake ground motions as input for the time history analysis.

The results indicate that all contact element models predict the pounding response of closely spaced structures which is in good agreement with each other. However, the values of impact element properties are sensitive to the few parameters used in the numerical models and hence should be investigated and used properly. This study clearly shows that the pounding result depends on the ground motion characteristics and the relationship between the buildings fundamental period.

Keywords: Seismic pounding; impact simulation models; spring-dashpot contact element; linear elastic structures; time history analysis.

1. INTRODUCTION

The phenomenon of pounding between buildings during earthquakes has been recently intensively studied by applying various structural models and using different models of collisions. Studies of seismic pounding typically employ the so called lumped mass model, where the building floors are assumed as diaphragms with lumped seismic masses. Early work in the idealization of the pounding phenomenon also utilized Single Degree-Of-Freedom (SDOF) oscillators in order to simplify the problem and produce some qualitative results on the behavior of structures under pounding. The numerical models are further simplified by employing two dimensional analyses and three dimensional analyses. The fundamental study on pounding between adjacent buildings in series was conducted by Anagnostopoulos (1988). In the analysis, structures are modeled by single-degree-freedom systems and collisions are simulated with the help of the linear viscoelastic model of impact force. Multi-degree-of-freedom (MDOF) models, with each storey's mass lumped on the floor level, are used to analyze earthquake-induced pounding between buildings of unequal heights in more detail. Maison and Kasai (1992), employed such models to study the response of light high-rise building colliding against a massive low rise structures. In the study, a single linear spring, placed at the roof level of the lower structure, was used to model the impact force during collision. Pantelides and Ma (1998), considered the dynamic behavior of damped SDOF elastic and inelastic structural systems with one-sided pounding during an earthquake using the Hertz contact model to capture pounding. Papadrakakis and Mouzakis (2004) have investigated the linear and nonlinear structural response for the three dimensional pounding phenomenon of two adjacent buildings during earthquakes with aligned rigid horizontal diaphragms. The developed formulation takes into account three dimensional dynamic contact conditions for the velocities and accelerations based on the impulse-momentum relationships, using the coefficient of restitution. Pant *et al.* (2010) have presented the three-dimensional (3D) simulation of seismic pounding between reinforced concrete (RC) moment-resisting frame buildings considering material as well as geometric nonlinearities.

The main intention of this paper is to study the pounding influence of adjacent structures with various available contact elements for impact simulation. The equation of motion for SDOF and MDOF

system for one side as well as both side pounding is being solved using a MATLAB program developed for this purpose. Few sets of solution obtained from the program are also compared with the SAP 2000 NL (Version-14) software results.

2. CONTACT ELEMENT MODELS

The contact element is linear or nonlinear based on the stiffness of spring element and the damping properties of dashpot. The stereomechanical model, which works on the principle of momentum conservation and coefficient of restitution, is rather not recommended when a precise pounding involved structural response is required especially in the case of multiple impacts with longer duration as suggested by Athanassiadou (1994). The stereomechanical approach uses the instantaneous impact for which the duration of impact is being very small, which is not true in the case of building pounding. Furthermore, this approach cannot be implemented in widely used commercially available software as mentioned by Papadrakakis (1991). Therefore, in the present work, the investigations are reported for the effect of contact elements on the impact response of the adjacent structures and are explained in the successive paragraph as well as a typical model of contact elements is shown in Figure 1.

2.1 Linear spring model

A linear impact of stiffness (k_i) can be used to simulate impact. The impact force is provided by

$$F_c(t) = k_1 \delta(t), \quad (2.1)$$

where, $\delta(t)$ is the interpenetration depth of the colliding bodies. This model is shown in Figure 1(a) which has been extensively used for impact simulation by Maison and Kasai (1990).

2.2 Kelvin-Voigt element model

The model shown in Figure 1(b) has been widely used by Anagnostopoulos (1988).

$$F_c(t) = k_k \delta(t) + c_k \dot{\delta}(t) \quad (2.2)$$

where, k_k is the spring linear stiffness of contact element, $\dot{\delta}(t)$ is the relative velocity between the colliding bodies at time t . the damping coefficient c_k can be related to the coefficient of restitution e , by equating the energy losses during impact:

$$c_k = 2\xi \sqrt{k_k \left(\frac{m_1 m_2}{m_1 + m_2} \right)} \quad (2.3)$$

$$\xi = -\frac{\ln e}{\sqrt{\pi^2 + (\ln e)^2}} \quad (2.4)$$

To avoid the tensile impact forces, slight modification is proposed by Komodromos (2007). The modified equation for the next time interval is written as

$$F_c(t + \Delta t) = \begin{cases} k_k \delta(t) + c_k \dot{\delta}(t) & F_c(t) > 0, \\ 0 & F_c(t) \leq 0. \end{cases} \quad (2.5)$$

2.3 The Modified Kelvin-Voigt element model

This model is developed by Pant (2010). Here, the impact force $F_c(t)$ is expressed as,

$$F_c(t + \Delta t) = \begin{cases} k_k \delta(t) + c_k \dot{\delta}(t) & \delta > 0 \text{ and } \dot{\delta} > 0, \\ k_k \delta(t) & \delta > 0 \text{ and } \dot{\delta} \leq 0, \\ 0 & \delta \leq 0 \end{cases} \quad (2.6)$$

Where, k_k is the stiffness of spring element, c_k is the damping coefficient and indentation at contact surface δ and relative velocity of impact $\dot{\delta}$.

$$c_k = \xi \delta, \quad \text{where, } \xi \text{ is damping ratio,} \quad \xi = \frac{3k_k(1-r^2)}{2r^2\dot{\delta}_0} \quad (2.7)$$

In which, r is the coefficient of restitution and $\dot{\delta}_0$ is the relative velocity just before the impact. This model is depicted in Figure 1(c).

2.4 Hertz contact element model

In order to model highly non-linear pounding more-realistically, Hertz impact model has been adopted by various researchers [Davis (1992) & Chau *et al.* (2003)].

The force in the contact element as shown in Figure 1(d) can be expressed as:

$$F_c = \left. \begin{cases} k_h \delta(t) & \delta(t) > 0, \\ 0 & \delta(t) \leq 0. \end{cases} \right\} \quad (2.8)$$

Where, $\delta(t)$ is the relative displacement. Assuming that the colliding structures are spherical of density ρ and the radius R_i estimation can be calculated from equation 2.9. [Goldsmith (1960)]:

$$R_i = \sqrt{\frac{3m_i}{4\pi\rho}}, \quad i = 1, 2 \quad (2.9)$$

The nonlinear spring stiffness k_h is linked to the material properties and the radii of the colliding structures as stated through the following formula:

where, h_1 and h_2 are the material parameters defined by the formula:

$$k_h = \frac{4}{3\pi(h_1 + h_2)} \left[\frac{R_1 R_2}{R_1 + R_2} \right]^{1/2} \quad (2.10)$$

$$h_i = \frac{1 - \gamma_i}{\pi E_i} \quad i = 1, 2 \quad (2.11)$$

Here, γ_i and E_i are the Poisson's ratio and Young's Modulus respectively. The coefficient k_h depends on material properties and geometry of colliding bodies.

2.5 Hertz damp contact element model

An improved version of the Hertz model, called Hertzdamp model, has been considered by Muthukumar and DesRoches (2006) wherein a non-linear damper is used in conjunction with the Hertz spring.

The pounding force for the model shown in Figure 1(e) is written as

$$\left. \begin{aligned} F(t) &= k_h \delta^{3/2} \left[1 + \frac{3(1-e^2)}{4(v_1 - v_2)} \dot{\delta}(t) \right]; & \delta(t) > 0 \\ F(t) &= 0; & \delta(t) \leq 0 \end{aligned} \right\} \quad (2.12)$$

Where, e is the coefficient of restitution and $\dot{\delta}(t)$ is the relative velocity during contact and $v_1 - v_2$ is the relative approaching velocities prior before contact.

2.6 Nonlinear viscoelastic model

Another improved version of the Hertz model has been introduced by Jankowski (2006) as shown in Figure 1(f). The contact force for this model is expressed as:

$$\left. \begin{aligned} F(t) &= \beta \delta^{3/2}(t) + \bar{c}(t) \dot{\delta}(t); & \delta(t) > 0 \text{ and } \dot{\delta}(t) > 0 & \quad \text{(Approach period)} \\ F(t) &= \beta \delta^{3/2}(t); & \delta(t) < 0 \text{ and } \dot{\delta}(t) < 0 & \quad \text{(restitution period)} \\ F(t) &= 0; & \delta(t) \leq 0 & \end{aligned} \right\} \quad (2.13)$$

Where, β is the impact stiffness parameter and $\bar{c}(t)$ is the impact element damping. Here ξ is an impact damping ratio corresponding to a coefficient of restitution e which can be defined as;

$$\xi = \frac{9\sqrt{5}}{2} \frac{1-e^2}{e(e(9\pi-16)+16)}$$

$$\bar{c}(t) = 2\xi \sqrt{\beta \sqrt{\delta(t)} \frac{m_1 m_2}{m_1 + m_2}}$$
(2.14)

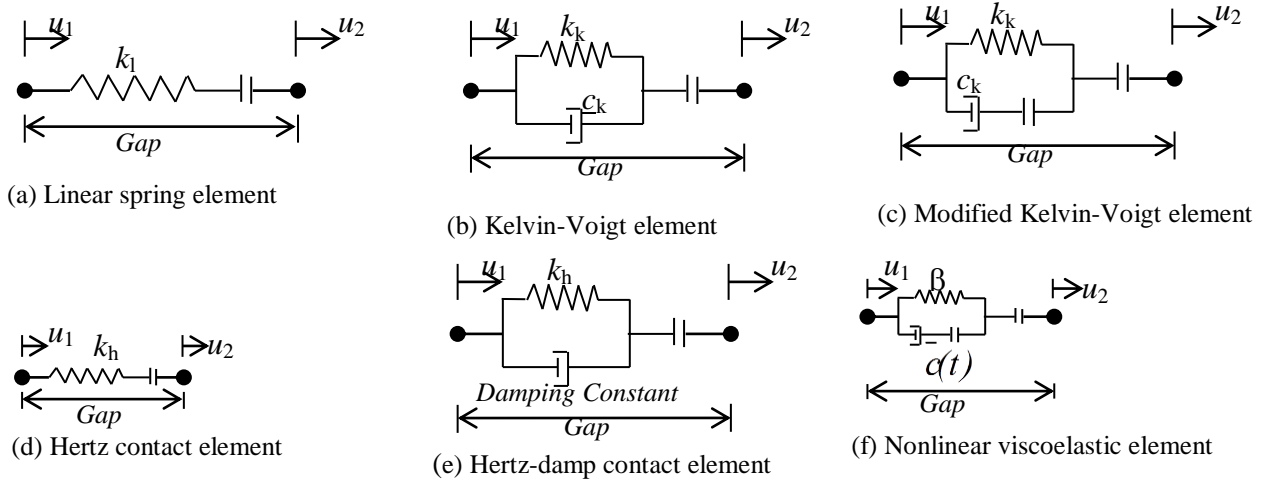


Figure 1. Contact elements for impact simulation

3. NUMERICAL MODEL

As an example, the study presented in this paper are focused on pounding between three adjacent fixed based linear elastic single-degree-of-freedom as well as multi-degree-of-freedom stick models by using existing various contact element approach for the impact simulation. The results of MATLAB program for analysis of SDOF and MDOF structure are verified using SAP 2000 NL.

3.1 SDOF and MDOF stick models

SDOF and MDOF stick models which are chosen for the studies are as below.

- i). Model I - With a linear spring element for impact simulation.
- ii). Model II - With a Kelvin-Voigt element model for impact simulation
- iii). Model III - With a modified Kelvin-Voigt element for impact simulation
- iv). Model IV – With a Hertz contact element for impact simulation
- v). Model V – With a Hertz-damp contact element for impact simulation
- vi). Model VI – With a Nonlinear Viscoelastic contact element for impact simulation.

The structural properties and gap element properties are chosen arbitrarily for the present work and which are specified below.

Structural Properties for SDOF structures-

$m_1 = 2500$ kg, $m_2 = 4500$ kg, $m_3 = 9800$ kg, $\omega_1 = 1$ Hz, $\omega_2 = 1.5$ Hz, $\omega_3 = 2$ Hz, damping ratio (ξ) = 5%, damping constant (c) = $2m\omega_n\xi$ and initial pounding force of structures $F_1(t) = F_2(t) = F_3(t) = 0$. Where, m_1 , ω_1 and $F_1(t)$ is the mass, natural frequency and initial impact force of left structures respectively as shown in Figure 2, similarly, m_2 , ω_2 and $F_2(t)$ and m_3 , ω_3 and $F_3(t)$ is the mass, natural frequency and initial impact force of middle and right structures respectively.

Structural Properties for MDOF structures-

$m_{11} = m_{21} = m_{31} = 10$ t, $k_{11} = k_{21} = k_{31} = 6000$ kN/m, $m_{12} = m_{22} = m_{32} = 15$ t, $k_{12} = k_{22} = k_{32} = 12000$ kN/m, $m_{13} = m_{23} = m_{33} = 20$ t, $k_{13} = k_{23} = k_{33} = 20000$ kN/m, Rayleigh mass and stiffness proportional damping is being used for calculating the damping constants.

Where, m_{11} , m_{21} and m_{31} is the mass at storey level 1, 2 and roof level of left building, similarly k_{11} , k_{21} and k_{31} is the stiffness of storey 1, 2 and 3 of left building. In the same manner the mass and stiffnesses of middle and right structures are taken randomly as shown in Figure 3.

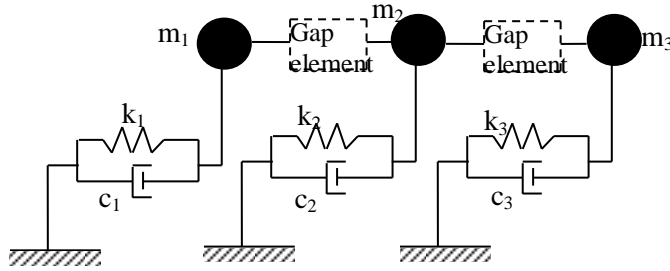


Figure 2: SDOF structures

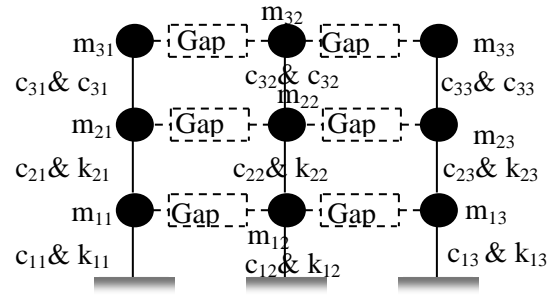


Figure 3: MDOF structures

Gap element properties for SDOF and MDOF structures–

The value of gap element stiffness is taken as 9740000 N/m [Jankowski (2006)] for Model I, II & III. In Model IV, V & VI the stiffness of gap element is calculated from Equation 9, 10 & 11. Separation distance of SDOF adjoining structures is considered constant as 0.01 m, whereas for MDOF structures, it is taken as 0.025 m at all storey levels. The Impact forces are calculated from the respective pounding force equation of each model.

The Characteristics of various real earthquakes used for the present study are given in Table 1. The output of the time history analysis is measured in terms of floor displacement and impact forces at the pounding levels for the maximum up to 10 seconds at an interval of 0.02 second.

Table 1. Characteristics of real earthquakes used for the present study.

| Captions of recorded ground motion | Year | Absolute acceleration component in terms of 'g' (9.81 m/s^2) | Duration (seconds) | Recorded station |
|------------------------------------|------|--|--------------------|------------------------|
| El Centro | 1940 | 0.313 | 31.6 | N-S component Terminal |
| Northridge | 1994 | 0.604 | 30 | Castaic old ridge |
| Kobe | 1995 | 0.629 | 36 | KMMO, Kobe, Japan |

4. RESULTS AND DISCUSSION

4.1 Validation of MATLAB program solution with SAP2000 results

Validation of MATLAB program for Model I of MDOF stick models of section 3 is carried out using SAP 2000 NL results.

Though SAP 2000 is having some limitations, but it can very easily reproduce the results for Model I with reasonably degree of accuracy. In the present paper, the comparative study between SAP 2000 and MATLAB for Model I of MDOF structures is presented in Figure 4 and 5. These results have given for top storey level pounding of left MDOF structure only.

After assessing the results of Figures 4&5, it is noted that the response obtained using SAP 2000 is in good agreement with the MATLAB program for Model I of MDOF left structure at top storey level collision. So for preliminary study of pounding in the complicated structure like plane frame structure and space frame structure, the SAP 2000 software is the good option for modeling the structures.

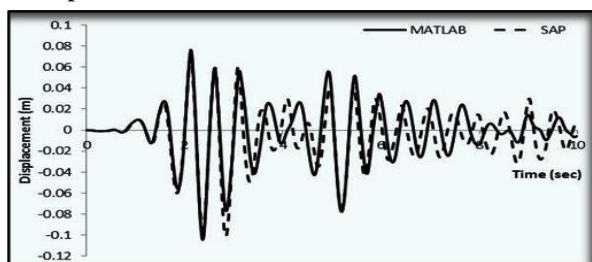


Figure 4: Top floor displacement comparison between SAP and Matlab results of left structure for Model I of MDOF system for to El Centro ground motion

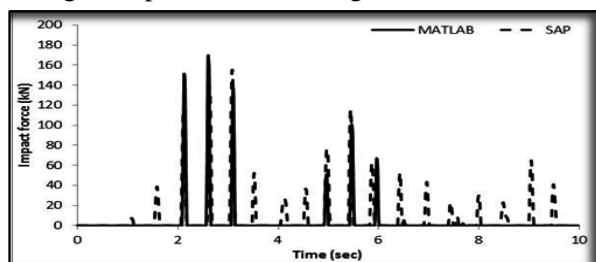


Figure 5: Top floor impact force SAP and Matlab results comparison between left and middle structure for Model I of MDOF system for El Centro ground motion

4.2 Comparative study of three adjacent SDOF structures for the various impact models

This section is entirely devoted to the comparative study of three adjacent SDOF structures for the various available contact elements used for the impact simulation. For the comparative study, the models, gap element properties and structural properties are mentioned in section 3. The results of comparative study are presented in the form of displacement and impact force time histories as shown in Figures 6 to 10 for El Centro ground motions. Also, the peak impact force and absolute displacement of time history plots due to various ground motion inputs are given in Table 2&3.

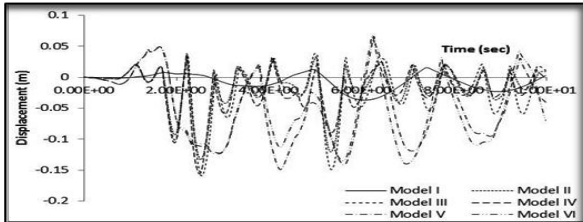


Figure 6: Floor displacement time history of left structure for El Centro ground motion input.

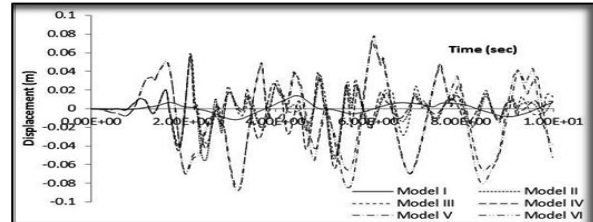


Figure 7: Floor displacement time history of middle structure for El Centro ground motion input.

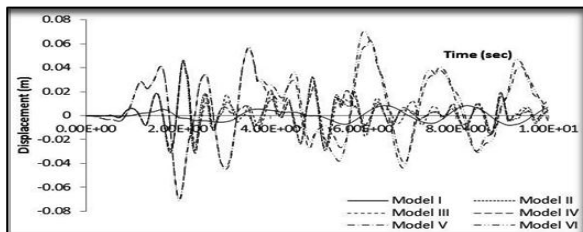


Figure 8: Floor displacement time history of right structure for El Centro ground motion input.

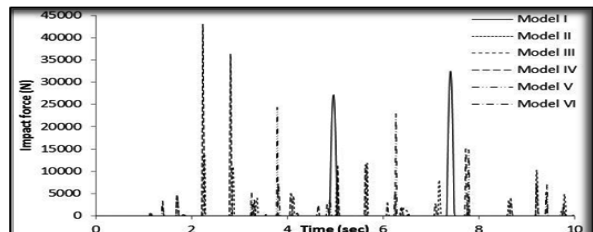


Figure 9: Impact force time history between left and middle structures for El Centro ground motion input.

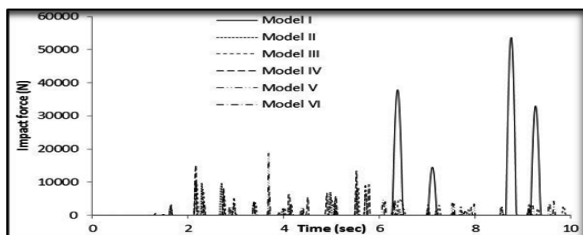


Figure 10: Impact force time history between middle and right structures for El Centro ground motion input.

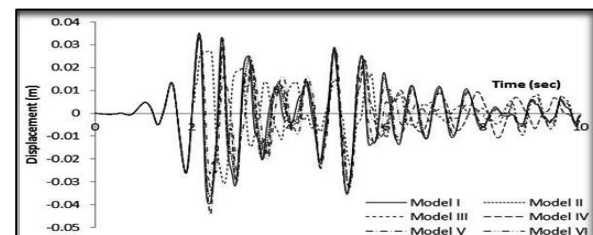


Figure 11: Floor displacement time history of left MDOF structure at first storey level for El Centro ground motion input.

Table 2. Peak Impact forces and number of impacts between the SDOF structures under various ground motions

| Models | Left and middle structures | | | | | | Middle and right structures | | | | | |
|-----------|----------------------------|----|------------|----|--------|----|-----------------------------|----|------------|----|--------|----|
| | El Centro | | Northridge | | Kobe | | El Centro | | Northridge | | Kobe | |
| | F (kN) | n | F (kN) | n | F (kN) | n | F (kN) | n | F (kN) | n | F (kN) | n |
| Model I | 32.5 | 16 | 109 | 25 | 41.8 | 22 | 53.7 | 41 | 53.7 | 41 | 19.2 | 21 |
| Model II | 7.8 | 28 | 28.7 | 29 | 33.6 | 30 | 10.2 | 47 | 17.5 | 56 | 23.7 | 55 |
| Model III | 8.9 | 37 | 26.1 | 26 | 48.2 | 28 | 9.54 | 70 | 18.2 | 74 | 40.7 | 64 |
| Model IV | 42.7 | 38 | 59.7 | 37 | 71 | 39 | 14.8 | 40 | 39.3 | 54 | 99.8 | 52 |
| Model V | 24.4 | 17 | 121.5 | 13 | 88.4 | 21 | 18.8 | 33 | 104 | 22 | 39.7 | 27 |
| Model VI | 15 | 18 | 50.7 | 16 | 75.6 | 23 | 6.88 | 31 | 31 | 33 | 37.8 | 26 |

F – Impact force, n – Number of impacts

It is observed from Table 2 that that Model I produce higher magnitude impact forces with lesser numbers of impacts than the Model II and III that's mainly due to absence of damping in the gap element. In Model II and III, responses are almost identical to each other. However, Model IV has a higher pounding force values with more numbers of impact than the Model V & VI except in

Northridge earthquake response since due to absence of damping term in the nonlinear gap element, which means it transferred energy more rapidly than any others during collision.

Table 3. Absolute displacements of SDOF structures under various ground motion inputs.

| Ground motion inputs | Absolute displacement in meters | | | | | | | | | | | | | | | | | |
|----------------------|---------------------------------|-------|-------|----------|-------|-------|-----------|-------|-------|----------|-------|-------|---------|-------|-------|----------|-------|-------|
| | Model I | | | Model II | | | Model III | | | Model IV | | | Model V | | | Model VI | | |
| | L | M | R | L | M | R | L | M | R | L | M | R | L | M | R | L | M | R |
| El Centro | 0.037 | 0.014 | 0.008 | 0.133 | 0.056 | 0.046 | 0.160 | 0.055 | 0.046 | 0.156 | 0.064 | 0.044 | 0.149 | 0.088 | 0.069 | 0.14 | 0.084 | 0.071 |
| Northridge | 0.10 | 0.023 | 0.021 | 0.211 | 0.103 | 0.070 | 0.244 | 0.104 | 0.062 | 0.230 | 0.137 | 0.065 | 0.59 | 0.274 | 0.202 | 0.418 | 0.271 | 0.176 |
| Kobe | 0.146 | 0.022 | 0.016 | 0.268 | 0.154 | 0.089 | 0.291 | 0.167 | 0.102 | 0.403 | 0.15 | 0.103 | 0.368 | 0.203 | 0.188 | 0.515 | 0.241 | 0.188 |

L – Left structure, M- middle structure and R – right structure.

From Table 3, it is observed that left structure undergoes more displacement than the adjoining structures due to its higher stiffness. It is also observed that the displacement responses are higher for Kobe earthquake than other two. After thorough observation of table, it is noted that the pounding response is depends on the gap element properties as well as on the input ground motion characteristics.

Thorough evaluation of Figures 6 to 8, it is observed that Model I have smooth displacement response than any other models. Model II & III displacement responses are reasonably matches with each other. Interestingly, it is observed from the Figures 6 to 8 that the displacement response of Model IV is comparable to Model II & III instead of Model V & VI since they have the same phase response. Model V & VI displacement response are moderately matches to each other as per as their phase difference are concerned the peak displacements are not exactly be the same, these two models have the maximum displacements than any other models because of nonlinearity/inelasticity of stiffness and damping of gap element.

After studying the Figures 9 & 10, it is noticed that Model I makes high magnitude impact forces than any others but their numbers of contact are exceptionally low. The time instant of peak impact forces of Model I, II & III are almost identical. In Model I, II & III, the peak collision forces remains intact for higher time interval nearly 1 to 1.5 seconds than any others but they are less frequent. From the same figures it is also noted that Model IV generates more and regular numbers of impact forces than any other models, whereas Model VI creates less magnitude but regular pounding forces between the adjoining structures.

4.3 Comparative study of three adjacent MDOF structures for the various impact models

For the comparative study, the MDOF models, gap element properties and structural properties are mentioned in section 3. The results of comparative study are presented in the form of displacement and impact force time histories as shown in Figures 11 to 25 for El Centro ground motions. Also, the absolute displacement and peak impact force values of time history plots due to various ground motion inputs are given in Tables 4 and 5.

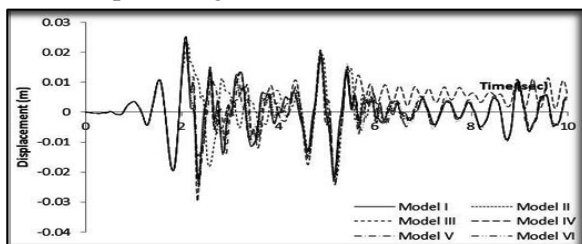


Figure 12: Floor displacement time history of middle structure at first storey level for El Centro ground motion.

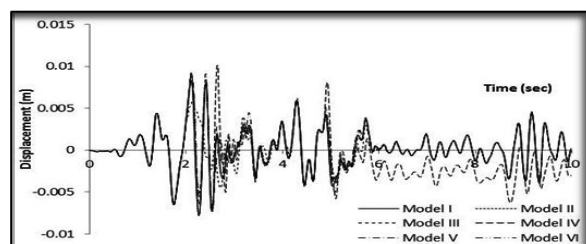


Figure 13: Floor displacement time history of right structure at first storey level for El Centro ground motion input.

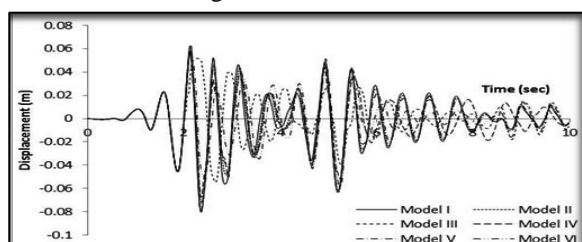


Figure 14: Floor displacement time history of left structure at second storey level for El Centro ground motion input.

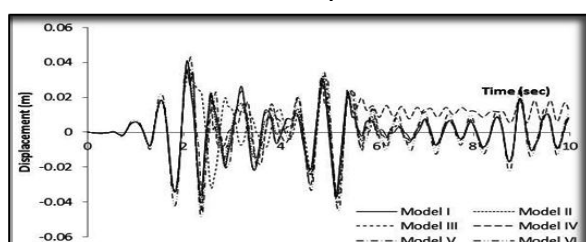


Figure 15: Floor displacement time history of middle structure at second storey level for El Centro ground motion input.

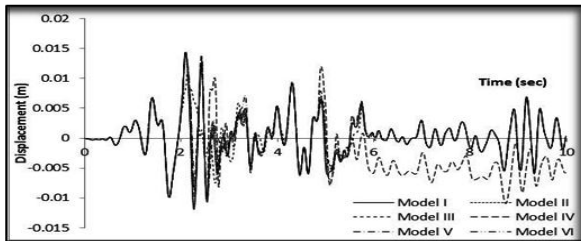


Figure 16: Floor displacement time history of right structure at second storey level for El Centro ground motion input.

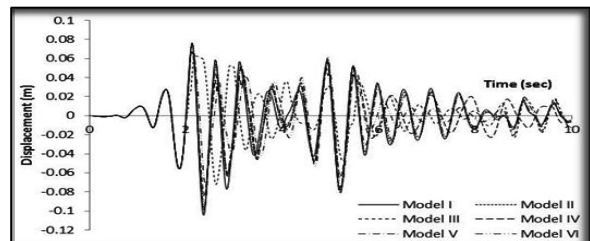


Figure 17: Floor displacement time history of left structure at third storey level for El Centro ground motion input.

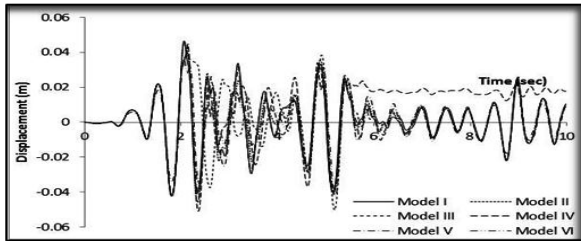


Figure 18: Floor displacement time history of middle structure at third storey level for El Centro ground motion input.

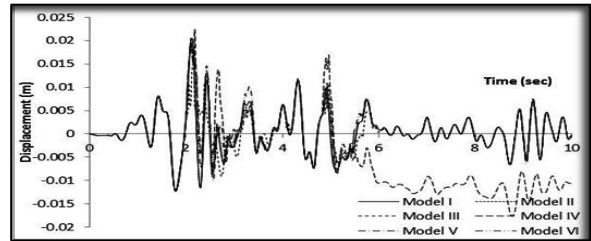


Figure 19: Floor displacement time history of right structure at third storey level for El Centro ground motion input.

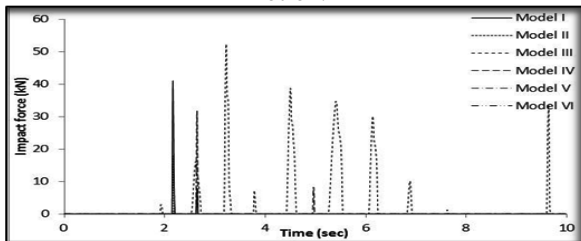


Figure 20: Impact force time history between left and middle MDOF structures at first storey level for El Centro ground motion input.

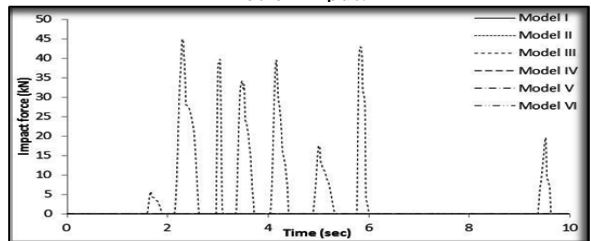


Figure 21: Impact force time history between middle and right MDOF structures at first storey level for El Centro ground motion input.

After evaluating the Figures 11 to 19, it is observed that the third storey displacement response is more transient than second and first storey subsequently. Interestingly it is observed from these figures is that the displacement response of all models are drastically changed with respect to each other in the time range of 2.3 to 6 second, whereas in the remaining time span it remains unchanged. It can be seen noted that the displacement response of Model IV is shifted from the main axis that means there is a permanent deformation in the structure due to the nonlinearity or inelastic properties of gap element.

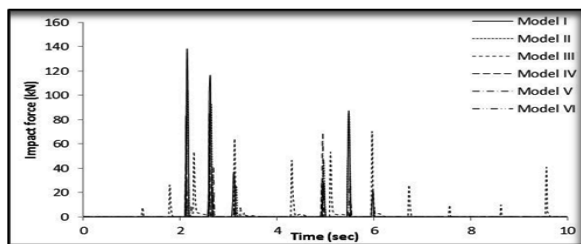


Figure 22: Impact force time history between left and middle MDOF structures at second storey level for El Centro ground motion input.

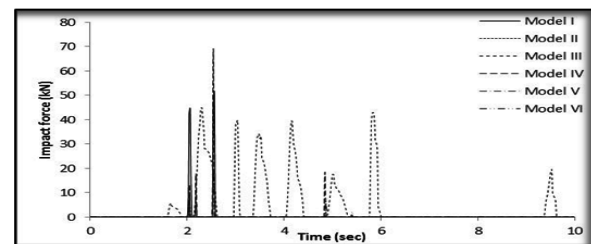


Figure 23: Impact force time history between middle and right MDOF structures at second storey level for El Centro ground motion input.

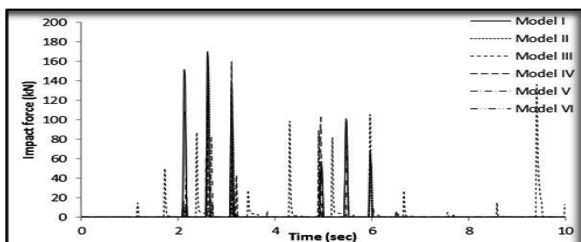


Figure 24: Impact force time history between left and middle MDOF structures at third storey level for El Centro ground motion input.

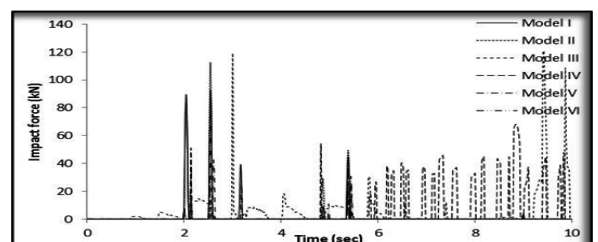


Figure 25: Impact force time history between middle and right MDOF structures at third storey level for El Centro ground motion input.

Table 4. Absolute displacements of MDOF structures under various ground motion inputs.

| Ground motion inputs | Absolute displacement in meters | | | | | | | | | | | | | | | | | |
|----------------------|---------------------------------|--------|--------|----------|-------|-------|-----------|-------|-------|----------|-------|--------|---------|--------|-------|----------|--------|-------|
| | Model I | | | Model II | | | Model III | | | Model IV | | | Model V | | | Model VI | | |
| | L | M | R | L | M | R | L | M | R | L | M | R | L | M | R | L | M | R |
| First storey level | | | | | | | | | | | | | | | | | | |
| El Centro | 0.039 | 0.0253 | 0.0083 | 0.036 | 0.025 | 0.008 | 0.031 | 0.022 | 0.006 | 0.033 | 0.029 | 0.010 | 0.044 | 0.024 | 0.009 | 0.033 | 0.0248 | 0.009 |
| Northridge | 0.061 | 0.038 | 0.015 | 0.057 | 0.040 | 0.015 | 0.034 | 0.033 | 0.009 | 0.052 | 0.036 | 0.016 | 0.046 | 0.0397 | 0.014 | 0.046 | 0.039 | 0.014 |
| Kobe | 0.059 | 0.064 | 0.017 | 0.050 | 0.038 | 0.016 | 0.050 | 0.034 | 0.015 | 0.061 | 0.040 | 0.017 | 0.052 | 0.036 | 0.018 | 0.052 | 0.036 | 0.018 |
| Second storey level | | | | | | | | | | | | | | | | | | |
| El Centro | 0.080 | 0.041 | 0.014 | 0.072 | 0.040 | 0.014 | 0.054 | 0.041 | 0.010 | 0.067 | 0.045 | 0.014 | 0.079 | 0.037 | 0.014 | 0.058 | 0.048 | 0.014 |
| Northridge | 0.111 | 0.065 | 0.022 | 0.106 | 0.069 | 0.022 | 0.058 | 0.037 | 0.014 | 0.092 | 0.064 | 0.0217 | 0.084 | 0.067 | 0.019 | 0.083 | 0.067 | 0.019 |
| Kobe | 0.109 | 0.064 | 0.021 | 0.082 | 0.062 | 0.025 | 0.084 | 0.062 | 0.025 | 0.103 | 0.065 | 0.025 | 0.092 | 0.061 | 0.026 | 0.092 | 0.061 | 0.026 |
| Third storey level | | | | | | | | | | | | | | | | | | |
| El Centro | 0.104 | 0.046 | 0.020 | 0.095 | 0.046 | 0.020 | 0.072 | 0.050 | 0.014 | 0.084 | 0.050 | 0.022 | 0.099 | 0.043 | 0.019 | 0.075 | 0.043 | 0.019 |
| Northridge | 0.146 | 0.077 | 0.026 | 0.137 | 0.081 | 0.026 | 0.071 | 0.071 | 0.02 | 0.11 | 0.076 | 0.033 | 0.104 | 0.076 | 0.040 | 0.104 | 0.076 | 0.040 |
| Kobe | 0.14 | 0.079 | 0.036 | 0.103 | 0.079 | 0.036 | 0.115 | 0.078 | 0.044 | 0.122 | 0.080 | 0.039 | 0.115 | 0.079 | 0.045 | 0.111 | 0.079 | 0.045 |

L – Left structure, M- middle structure and R – right structure.

Table 5. Peak Impact forces between the MDOF adjacent structures under various ground motion inputs

| Storey level | Ground motion inputs | Peak impact forces in kN | | | | | | | | | | | |
|--------------|----------------------|--------------------------|-------|----------|-------|-----------|-------|----------|-------|---------|-------|----------|-------|
| | | Model I | | Model II | | Model III | | Model IV | | Model V | | Model VI | |
| | | L-M | M-R | L-M | M-R | L-M | M-R | L-M | M-R | L-M | M-R | L-M | M-R |
| First | El Centro | 41 | 0 | 18.4 | 0 | 52.4 | 45 | 31.7 | 0 | 0.86 | 0 | 0 | 0 |
| | Northridge | 142.4 | 85.9 | 112.2 | 84.4 | 23.48 | 0 | 21.2 | 2.97 | 157 | 0 | 157 | 0 |
| | Kobe | 169.8 | 0 | 78.6 | 80.9 | 73.7 | 40.5 | 91 | 65.8 | 28.9 | 31.5 | 28.9 | 31.5 |
| Second | El Centro | 138 | 51.2 | 104 | 64.7 | 70.2 | 85.7 | 85.2 | 69.3 | 83.2 | 13 | 68.5 | 18.9 |
| | Northridge | 321.8 | 212.4 | 263.4 | 230.4 | 136.7 | 465.4 | 142.9 | 69.4 | 74.3 | 140.9 | 74.3 | 140.9 |
| | Kobe | 304.3 | 237.5 | 210.5 | 206.3 | 206 | 104 | 201.9 | 65.3 | 161.7 | 117.4 | 161.7 | 117.4 |
| Third | El Centro | 168.7 | 92.3 | 154.2 | 113 | 134.6 | 120.9 | 159.6 | 68.2 | 60.9 | 41.8 | 102.8 | 78.4 |
| | Northridge | 375.2 | 222.8 | 395.4 | 238.8 | 350 | 93.8 | 272.3 | 94.8 | 170.7 | 415 | 170.7 | 415 |
| | Kobe | 368.7 | 223.1 | 247.1 | 217.2 | 350 | 211 | 660 | 243.8 | 365.6 | 127.1 | 365.6 | 127.1 |

L-M: Between left and middle structure, and M-R: Between middle and right structure.

It can be observed from Table 4 that the left structure undergoes more displacement than the adjoining structures due to its higher stiffness. The displacement response increases from bottom toward the top of the structure as expected. After reviewing Table 3, it can say that Model I produce higher magnitude impact forces than any other models that’s mainly due to absence of damping in the gap element. Model V and VI impact force response are almost identical to each other. In general, the first storey experiences less pounding forces than second and third storey. Overall it is observed that the pounding response is depends on the gap element properties as well as on the input ground motion characteristics.

After studying the Figures 20 to 25, it is noticed that Model I, III and IV introduces much higher magnitude collision forces than any other models. Among all the models, Model III generates more numbers of impact forces. Higher storey experiences high magnitude and more number of pounding forces than the lower ones. From these figures it is recognized that the middle and right structures undergoes into plastic deformation in Model III & IV, that’s why the impact force remain present for quite a long time span (that is over 0.2 second or more approximately). It is also examined that the gap elements between left and middle structures initiated higher magnitude impact forces with more numbers than the gap elements of between middle and right structures in entire models.

6. CONCLUDING REMARKS

The behavior of three adjacent single-degree-of-freedom and multi-degree-of-freedom structures with existing linear and non linear contact element for impact simulation is investigated under earthquake excitation, assuming a linear elastic behavior of the structures. The governing equation of motion of SDOF stick models are formulated and solved using MATLAB program, which are also verified

using FE analysis package, SAP 2000 NL. Based on the trends of the result obtained from the numerical study following precise conclusions can be made:

- i. Pounding is a highly nonlinear phenomena and a severe load condition that could results in significant structural damage, high magnitude and short duration floor acceleration pulses in the form of short duration spikes, which in turns cause greater damage to the building components. A sudden break of displacement at the pounding level results in large and quick acceleration pulses in the opposite direction. This effect is even severe in the structures subjected to both side pounding incidences.
- ii. The results indicate that all contact element models predict the pounding response of closely spaced structures up to some reasonable limit of actual problem provided that the values of impact element properties should be investigated and used properly.
- iii. This study clearly shows that the pounding results depend on the ground motion characteristics and the relationship between the buildings fundamental period.
- iv. For the studied elastic structures, the phenomenon of rebound is not present therefore the pounding effect consists only be the transfer of energy between the structures.
- v. The modified Kelvin-Voigt element, Hertz element, Hertz-damp element and Nonlinear viscoelastic element cannot be easily implemented in available commercial software, So therefore adjacent structures needs to be analyzed by developing a program separately for the accurate prediction of pounding response.

REFERENCES

- Anagnostopoulos, S. A. (1988). Pounding of buildings in series during earthquakes. *Earthquake Engineering and Structural Dynamics*. **16**, 443-456.
- Athanassiadou, C. J., Penelis, G. G. and Kappos, A. J. (1994). Seismic response of adjacent buildings with similar or different dynamic characteristics. *Earthquake Spectra*. **10:2**, 293-317.
- Chau, K. T., Wei, X. X., Guo, X. and Shen, C. Y. (2003). Experimental and theoretical simulations of Seismic poundings between two adjacent structures. *Earthquake Engineering and Structural Dynamic*. **32**, 537-554.
- Davis, R. O. (1992). Pounding of buildings modeled by an impact oscillator. *Earthquake Engineering and Structural Dynamics*. **21**, 253-274.
- Goldsmith, W. (1960). Impact: The theory and physical behavior of colliding solids, First edition, Edward Arnold, London, England.
- Jankowski, R. (2006). Pounding force response spectrum under earthquake excitation. *Engineering Structures*. **28**, 1149-1161.
- Komodromos, P., Polycarpou, P. C., Papaloizou, L. and Phocas, M. C. (2007). Response of seismically isolated buildings considering poundings. *Earthquake Engineering and Structural Dynamics*. **36**, 1605-1622.
- Maison, B. F. and Kasai, K. (1990). Analysis for type of structural pounding. *ASCE Journal of Structural Engineering and Structural Dynamics*. **116:4**, 957-977.
- Maison, B. F. and Kasai, K. (1992). Dynamics of pounding when two buildings collide. *Earthquake Engineering and Structural Dynamics*. **21**, 771-786.
- Mouzakis, P. and Papadrakakis, M. (2004). Three dimensional nonlinear building pounding with friction during earthquakes. *Journal of Earthquake Engineering*. Imperial College Press **8:1**, 107-132.
- Muthukumar, S. and DesRoches, R. (2006). A hertz contact model with nonlinear damping for pounding simulation. *Earthquake Engineering and Structural Dynamics*. **35**, 811-828.
- Pantelides, P. and Ma, X. (1998). Linear and nonlinear pounding of structural systems. *Computers & Structures*. **66:1**, 79-92.
- Pant, R. and Wijeyewickrema, A. C. (2010). Seismic pounding between reinforced concrete buildings: A study using recently proposed contact element models. *Proc. of Fourteenth European Conference on Earthquake Engineering*. Ohrid, Republic of Macedonia (August-September 2010).
- Papadrakakis, M., Mouzakis, H., Plevris, N. and Bitzarakis, S. (1991). A lagrange multiplier solution method for pounding of buildings during earthquakes. *Earthquake Engineering and Structural dynamics*. **20**, 981-998.
- SAP User's Manual (Structural Analysis Program) (1995). Computers and Structures Inc., University Ave., Berkeley, CA.